한국해양공학회지 제21권 제5호, pp 9-17, 2007년 10월 (ISSN 1225-0767)

Performance Prediction of Impulse Turbine System in Various Operating Conditions

BEOM-SOO HYUN*, JAE-SEUNG MOON**, KEYYONG HONG** AND SEOK-WON HONG**

*Division of Naval Architecture and Ocean Systems Engineering, Korea Maritime University, Busan, Korea
**Maritime and Ocean Engineering Research Institute, KORDI, Daejeon, Korea

KEY WORDS: Wave energy, Impulse turbine, Compu fa fional fluid dynamics chart, Quasi-steady, Unsteady, Non-uniformity

ABSTRACT: *This paper deals with the design and analysis of a 250 kW class impulse turbine for wave energy conversion. Numerical analysis was performed using FLUENT. The size and the performance of a turbine required to provide a certain power can be estimated using a series of performance charts built through the present study. Temporal and spatial variations of flow fields were also considered and compared with those of uniform inflow. It was concluded that a simple steady-flow analysis using performance charts still provided a practical and useful way to predict the design and performance of turbines.*

1. Introduction

Impulse turbines installed on OWC chambers are considered one of the best wave-energy-extracting devices suitable for full-scale application, especially because of its wide operating range and relatively low rotational speed. As an example of full-scale turbine, a 250 kW-class impulse turbine was chosen to analyze the aerodynamic performance of internal duct flow around a turbine rotor as well as the whole air flow passage. The basic turbine model of Setoguchi et al. (2001) was employed for CFD calculation in a systematic manner for flow analysis with and without the turbine rotor.

Figure 1 is a typical example of OWC-type wave energy chamber with an impulse turbine inside a nozzle. Turbine performance depends not only on the specifications of the turbine itself, but also on the size of chamber, the incident wave conditions and the nozzle ratio. The scale effect between the model and the prototype turbines is another issue for the prediction of prototype turbine's performance. This paper deals with a global methodology for the analysis of model and/or prototype impulse turbines in various operating conditions.

In order for field engineers and designers to estimate system performance more easily, a steady flow analysis at a high Reynolds number was made to obtain the performance charts for the mean velocity field inside the duct, turbine power and pressure drop under various operating conditions.

교신저자 현범수: 부산시 영도구 동삼동 한국해양대학교
051-410-4308 bshyun@hhu.ac.kr

The inflow was assumed to be steady and the nonuniform effect created by the specific air chamber and duct assembly was considered separately.

Next, a quasi-steady analysis was made for the sinusoidally reciprocating air flow generated by wave elevation and

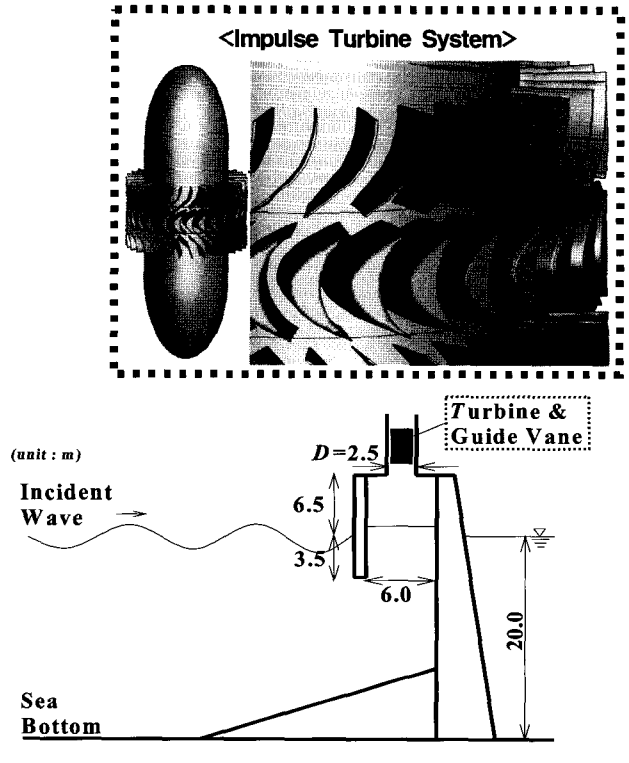

Fig. 1 Schematics of the prototype wave energy conversion system

compared to the results from the steady analysis. An unsteady analysis was also made for a reciprocating air flow inside the air chamber and duct in the absence of a turbine rotor in order to evaluate the stability and effectiveness of the air flow passage. Finally, the linearly varying shear flow and the parabolic flow at the inlet of the turbine rotor were applied instead of uniform inflow in order to see the effect of flow non-uniformity on turbine performance. The performance of the prototype impulse turbine was systematically evaluated at the various design stages so the effect of air flow passage as well as the temporal and spatial variations of flow could be indirectly corrected using the present analysis results.

2. Turbine Model, Numerical Method and Test Condition

Duct flow analysis with and without a turbine rotor for wave energy conversion was made with a basic turbine model from Setoguchi et al. (2001), which was known to be one of the best impulse turbines ever designed. An impulse turbine rotor with the diameter (D) of 38 cm contains 30 rotor blades (z = 30) and has a hub ratio of 0.7. Blade axial chord (l_r) and span (b) are 6.84 cm and 5.7 cm, respectively. Figure 2 shows the turbine geometry and provides some dimensions. More details can be found in Hyun and Moon (2004). G/l_r, denoting the gap between rotor and guide vane, is 0.19.

A full-scale turbine of the 250 kW-class was designed by adopting the same turbine introduced above and adjusting the scale of model turbine at the range of 0.5~2.5 m in diameter (Hong, 2005). Flow around the turbine was assumed steady for basic calculation in order to study the scale effect of the turbine, and the quasi-steady analysis was applied for the calculation in the sinusoidally reciprocating flow field. The unsteady calculation was employed for the precise unsteady analysis of the duct flow in the absence of the turbine. Here, the term "steady" means the rotor rpm and nozzle inflow are assumed to be constant, while "quasi-steady" allows for the change of inflow from wave motion and does not neglect any unsteady effect. "Unsteady" allows for all interactions between inflow and turbine in a real situation.

The whole turbine system was modeled as shown in Fig. 1 in order to predict of turbine performance in non-uniform flow conditions because the periodic flow conditions for turbine blade and guide vane could no longer be applicable.

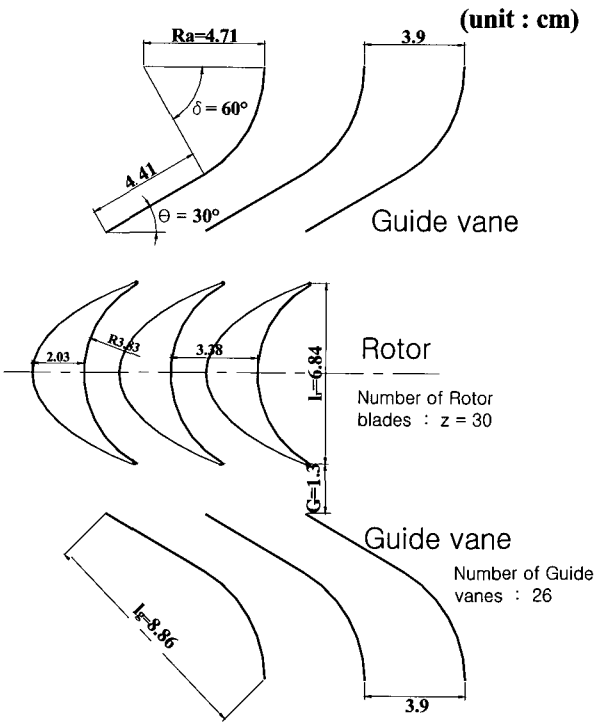

Fig. 2 Turbine geometry

FLUENT 6.1.22 was employed for the present three-dimensional analysis, while GAMBIT 2.1.6 was used for grid generation. An unstructured grid system using a tetrahedral mesh was adopted. Since it is very important to capture the detailed flow structure in the narrow gap between rotor tip and duct, where an unstructured grid works poorly, multiple layers of Cooper-type mesh were introduced for turbine calculation. A structured grid system was adopted for the flow field in the air chamber and duct in the absence of a turbine rotor because of simple geometry as well as effective resolution of the duct surface. The dependency of the grid on numerical accuracy has also been checked previously (Hyun and Moon, 2004). The k-ε model was employed for turbulent flow (Hong, 2004). Although turbine inflow was assumed basically to be sinusoidal, steady, quasi-steady or unsteady analyses were made depending on the purpose of the study. A relative moving reference frame was adopted for the rotor part of the impulse turbine. The range of blade Reynolds number varied from 10^5~2.5×10^6, where the Reynolds number was defined based on blade chord (l_r), the mean axial velocity and the kinematic viscosity of air (ν). More details can be found in Hong (2005).

Performance of the impulse turbine in the steady flow condition is expressed in terms of the input coefficient C_A and the torque coefficient C_T as follows;

$$C_A = \frac{\Delta pQ}{\frac{1}{2}\rho_a (v_a^2 + U_R^2) b l_r z v_a} \tag{1}$$

$$C_T = \frac{T}{\frac{1}{2}\rho_a (v_a^2 + U_R^2) b l_r z r_m} \tag{2}$$

Here Δp, Q, T represent pressure drop, flow rate and torque, and v_a, U_R, r_m are axial mean velocity, rotational velocity of rotor blade at $r = r_m$ and radius at mid-span, respectively. The efficiency of the turbine η and the flow coefficient ϕ can be expressed as follows:

$$\eta = \frac{T\omega}{\Delta pQ} = \frac{C_T}{C_A \phi} \tag{3}$$

$$\phi = \frac{v_a}{U_R} \tag{4}$$

where flow coefficient ϕ has a physically equivalent meaning with the angle of attack in wing theory, and ω is the angular velocity of the turbine rotor.

3. Scale Effect on the Performance of Prototype Turbine

The performance of the impulse turbine is commonly expressed by the efficiency and input/torque coefficients with respect to the flow coefficient, and it is customary to exclude the scale effect between model scale and prototype turbines because of the lack of full-scale data. Since the model-scale results are limited by Reynolds scaling in predicting the performance of the prototype, it is important to consider the effect of the Reynolds number for the prototype turbine as follows.

$$C_A = f(\phi, Re) \tag{5}$$

$$C_T = f(\phi, Re) \tag{6}$$

$$\eta = f(\phi, Re) \tag{7}$$

where $Re = \sqrt{v_a^2 + U_R^2}\, l_r / \nu$

The performance of the impulse turbine was calculated at various Reynolds numbers to account for the change of the turbine size. For the construction of a suitable grid system for high Reynolds number flow of $Re > 10^6$, the near-wall grid system was carefully adjusted based on the wall function approach applied.

Figure 3 shows the effects of the Reynolds number on input and torque coefficients although their effects are not dramatic. Input coefficient decreases with increasing Re for almost all ranges of flow coefficients, suggesting less of a pressure drop for higher Re. The effect on the torque coefficient was not visible; consequently, the turbine efficiency increases up to about 7% with increasing Re.

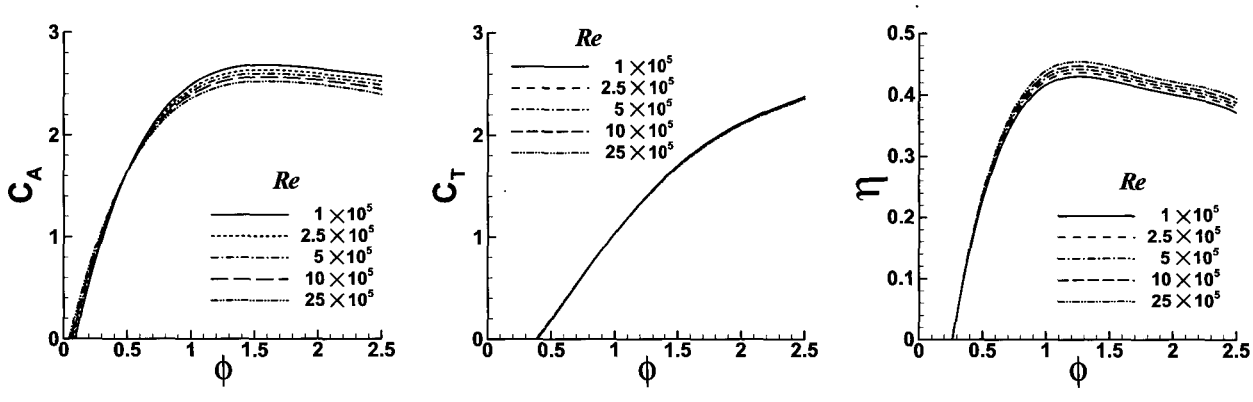

(a) Input coefficient, C_A (b) Torque coefficient, C_T (c) Turbine efficiency, η

Fig. 3 Variation of impulse turbine performance with respect to flow coefficient

4. Performance Chart for Prototype Turbine

In order to predict the size and the performance of a 250 kW-class turbine, the series of performance charts of turbine was prepared to allow quick estimates of the turbine system in the preliminary design stage and for ease of use by the field engineers. This is in keeping with the principle to obtain the combination of design parameters of the proposed turbine system at the level of power demand required by user with the prescribed flow rate (i.e., the mean axial velocity) at the inlet of the turbine rotor, which can be easily calculated from the wave elevation in the OWC chamber. A somewhat similar approach can be found in Thakker and Hourigan (2004). For the purpose of brevity, only two performance charts with two different turbine diameters are shown in Fig. 4 among five sets of charts constructed for the present study to cover the entire range of possible designs considered. Design ranges are as follows;

Mean axial velocity in a duct v_a	20~50 m/s
Number of Revolution of Turbine Rotor	400~1000 rpm
Diameter of Turbine Rotor D	0.5~2.5 m

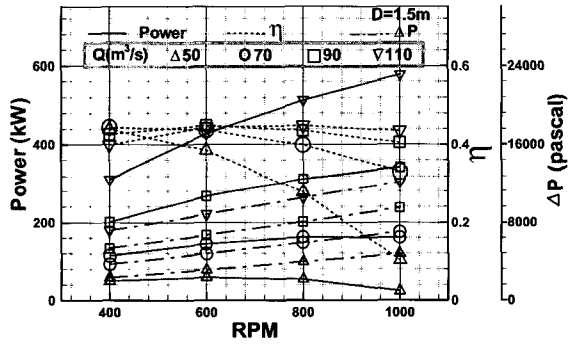

(a) D = 1.5 m

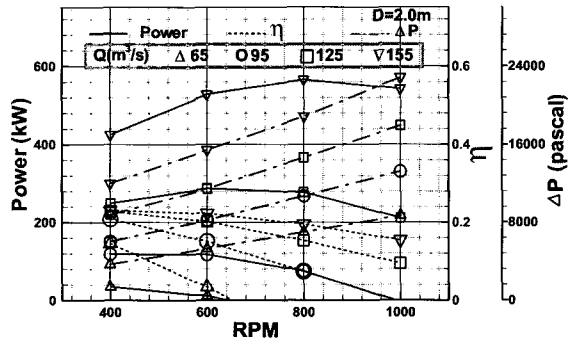

(b) D = 2.0 m

Fig. 4 Example of turbine performance chart

The typical procedure of using this chart is as follows; first air flow rate at nozzle, Q, is calculated based on wave motion inside a chamber. Then the turbine rotor rpm is usually set to a certain operating range depending on the optimum efficiency point and the specifications of the generator (Rotor rpm is not a constant; it is a variable according to wave condition.). With one Q and one rpm, the pressure drop, turbine efficiency and turbine power are obtained using data in Fig. 4. This process can be repeated by changing the turbine diameter or the air flow rate until the proper operating condition is found.

Figure 4 excludes the effects of unsteadiness and non-uniformity of duct inflow, and so is applicable only for the steadily rotating rotor and guide vanes in uniform flow. More details can be found in Hong (2005).

5. Quasi-steady Analysis of Turbine in Sinusoidal Flow

The turbine rotates in the unsteady flow field according to varying amplitudes and frequencies of ocean waves. Since the wave frequency is low enough compared to the turbine's rotor frequency, their interaction could be neglected, providing a justification for quasi-steady analysis (Hyun et al., 1992). Here, we have compared the possible differences between steady and quasi-steady calculations. Inflow was assumed sinusoidal in the quasi-steady case, while it is the mean axial velocity of sinusoidal flow in the steady case.

Figure 5 shows the curves for axial velocity, flow rate, pressure drop, torque, input and torque coefficients and efficiency calculated during one wave period. This example is quasi-steady result for D = 0.38m, v_a = 15 m/s and ϕ = 1 in a time-averaged sense, since one wave period was assumed to be 8 seconds. The input coefficient has a plateau shape most of the time. The torque coefficient is locally negative at a relatively low axial velocity and shows a somewhat different pattern from the others. The torque coefficient is actually not obtainable when the instantaneous axial velocity is zero; as a result, the turbine efficiency shows nearly steady values at most time periods, with some exceptions around zero instantaneous axial velocity. This is generally acceptable, but may contain some errors because of the assumption that the rotor speed is constant, while it usually varies with varying axial velocity. Therefore, it is expected that the abrupt change of efficiency does not occur in a real situation.

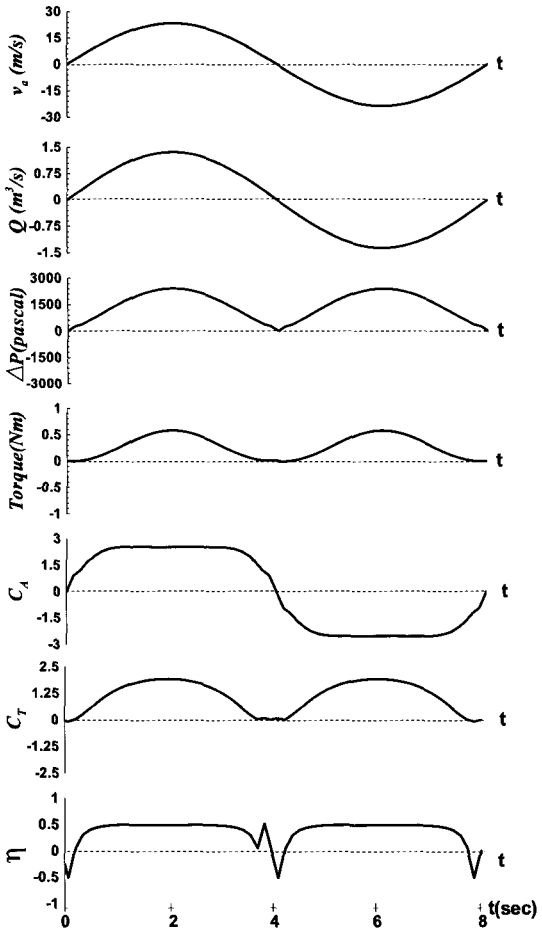

Fig. 5 Typical results of quasi-steady analysis

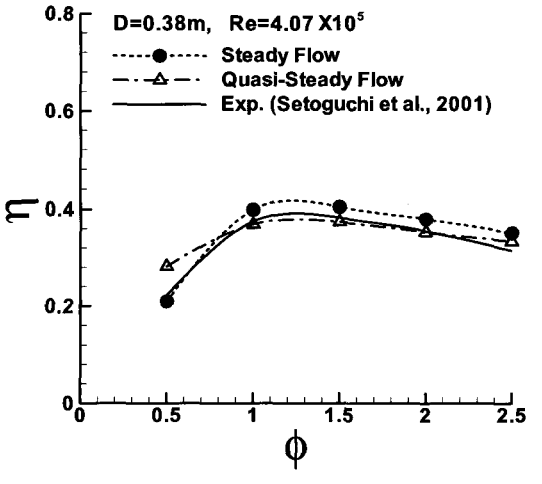

Fig. 6 Comparison between mean and quasi-steady analysis

Figure 6 compares the quasi-steady result to the steady one and to the experimental data of Setoguchi et al. (2001). The turbine efficiency for the quasi-steady case becomes a little lower at most of ϕ, while it is higher at relatively high rotational speeds (i.e., smaller ϕ). Although the quasi-steady result coincides with the experimental data better (except for smaller ϕ), it is reasonable to conclude that the differences among them are rather minor, so the steady calculation can be a fair prediction tool in general.

6. Unsteady Analysis of Duct Flow in the Absence of a Turbine Rotor

Calculation of a reciprocating flow inside a duct has usually been limited to steady or quasi-steady analyses because of the complexity of unsteady calculation. The present unsteady calculation for the flow field in an air chamber and duct system including elbows is made in the absence of a turbine rotor in order to understand the real unsteady flow phenomena and to complement the steady or quasi-steady analysis. A user-defined function (UDF) of FLUENT was utilized for the simulation of sinusoidal flow generated by the assumed wave motion.

The test model contained assumptions as follows; The air chamber has a diameter of 2.85 m, and the nozzle ratio of the duct is 1.78%. The total length of the duct system with an elbow is 7.8 m. The Reynolds number based on duct diameter and velocity is 4.07×10^5. The mean axial velocity in the duct and the wave period are assumed to be 5 m/s and 2 seconds, respectively. The calculating condition, then, is not the real situation, but an assumed condition used to evaluate the effect of unsteadiness in the simplest way. Therefore, the wave period is set shorter than the usual wave period at sea in order to exaggerate the effect of unsteady flow. With nozzle ratio as an important factor, the rest of the sizes were decided based on the concept of minimizing the calculation time. Figure 7 shows the flow patterns in the air chamber and duct in two typical cases. t* denotes dimensionless time - the total time duration divided by the incident wave period. For example, t* = 2.25 is the time after 2.25 time period of the incident wave.

Flow development with time was thoroughly examined by calculating the instantaneous flow field at a minimum of 8 time steps per one wave period. With a very small nozzle ratio, the flow inside the air chamber was found to be unstable because of sudden expansion and contraction, although the flow in a duct was much stable. Figure 7(a) is at the exhalation stage (flow from chamber to duct), while Fig. 7(b) is at the inhalation stage (flow

from outside to duct). Although both figures would have been the same if the quasi-steady assumption had been applied, the different flow pattern was obtained because of flow unsteadiness. Still, the flow inside a duct exhibits little difference between inhalation and exhalation phases, primarily because of the high contraction ratio. More investigations (not shown here) found little difference regardless of various duct parameters, such as duct shape, elbow, and length of duct. While the blockage effect between inhalation and exhalation phases may not be ignored, a tentative conclusion is that the flow can be modulated to be stable so the effect of unsteadiness on turbine performance is negligible, in spite of the unstable and unsteady flow conditions in the air chamber. The flow will be more stable in real at-sea situations, where wave period is much greater than 2 seconds. Figure 8 shows the velocity field at several stations, while Fig. 9 concentrates on more detailed velocity profiles inside the nozzle. In this calculation, the boundary condition of the fixed flow rate at each outlet was applied for the sinusoidal flow. The calculation domain was also invariant. The flow inside the nozzle is relatively uniform, except at the near-wall region before approaching the elbow. The elbow effect is limited to within 5 diameters from the elbow for both exhalation and inhalation. The present calculation condition is, in principle, different from the experiment performed by Setoguchi et al. (2003), where a piston used in the experiment experienced more external force as a result of the increase of pressure inside a chamber in the exhalation process, and vice versa. That is, the supply of pneumatic energy during inhalation should be higher than that during exhalation because of the loss of piston power. Thus, a direct comparison between experiment and calculation requires special care. For a proper comparison, more numerical investigations need to be made using an MDM (Moving & Deforming Mesh) option for a piston and proper boundary conditions.

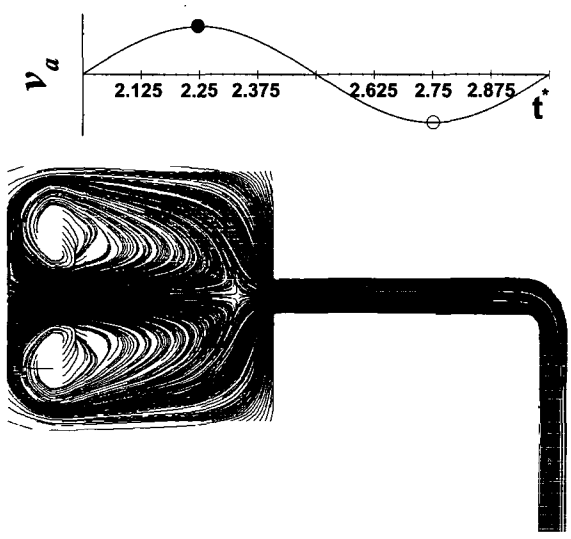

(a) $t^* = 2.25$ (Exhalations)

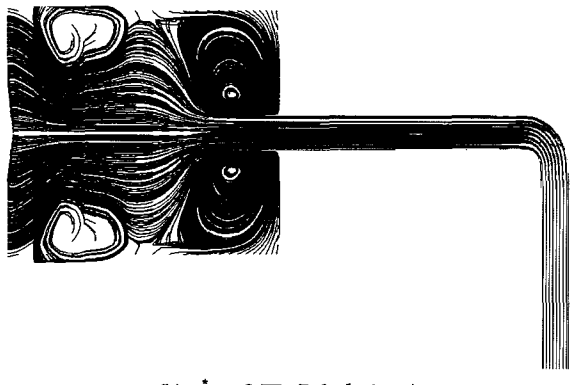

(b) $t^* = 2.75$ (Inhalations)

Fig. 7 Example of pathlines in air flow passage

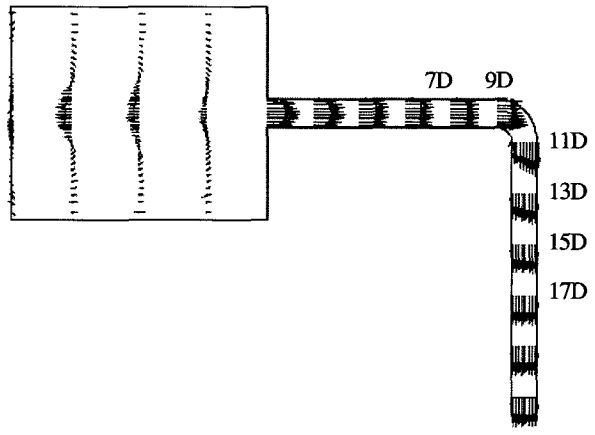

(a) $t^* = 2.25$ (Exhalations)

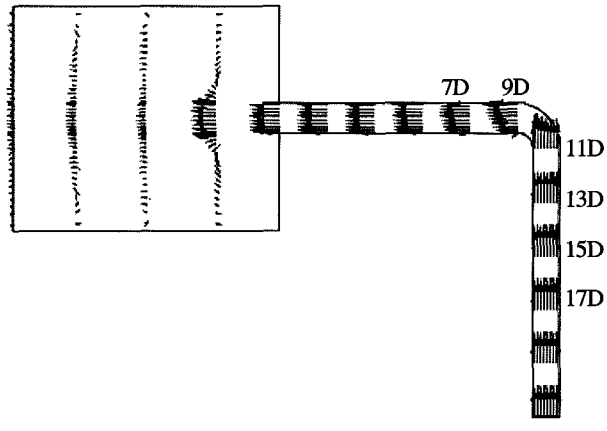

(b) $t^* = 2.75$ (Inhalations)

Fig. 8 Velocity vectors at several stations

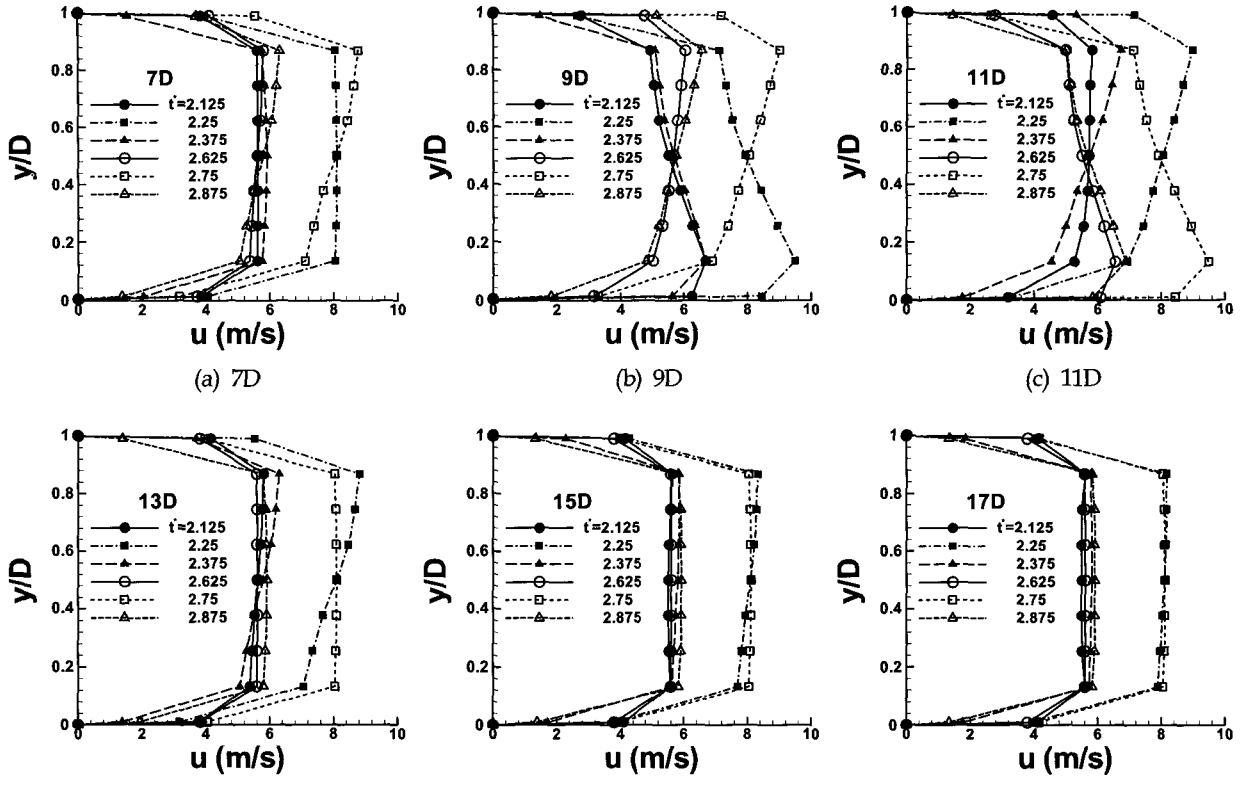

(a) 7D (b) 9D (c) 11D

(d) 13D (e) 15D (f) 17D

Fig. 9 Velocity profiles at various stations inside nozzle

7. Effect of Non-uniform Inflow on Turbine Efficiency

A duct system is usually not a straight duct, but an assembly of various pipes and elbows depending on the viewpoints of space allocation, overall maintenance and convenient connection with the generator. The length of the duct is also variable according to space limitations. Because of these kinds of effects, the inlet flow condition to the turbine can become non-uniform. The effect of non-uniform inlet conditions on turbine performance is considered by investigating the two typical inlet conditions: Linear shear flow and parabolic flow. A steady calculation was made using the mean axial velocity.

Figure 10 demonstrates the turbine performance for such inlet conditions, together with uniform flow condition. In terms of torque, the parabolic flow case offers rather less C_T, and nearly the same results for the uniform and linear shear cases. Pressure drop is highest for the uniform flow condition and lowest for the parabolic flow condition, although the difference is not large. Consequently, turbine efficiency becomes almost the same in all three cases. Since turbine performance is not much affected by the inflow of idealized extreme conditions, it is likely that the effect of non-uniform inflow is minor. The same is true for the result obtained using a case of actual duct flow with the worst non-uniformity calculated in a previous section.

8. Conclusions

Numerical analyses of the 250 kW-class impulse turbine were made. The size and performance of turbine required to meet a certain power demand can be estimated using a series of performance charts built through the present study. The temporal and spatial variations of flow field were considered to compare with those of uniform inflow. The results of the present study are summarized as follows:

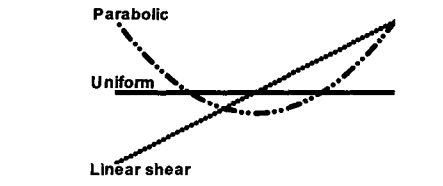

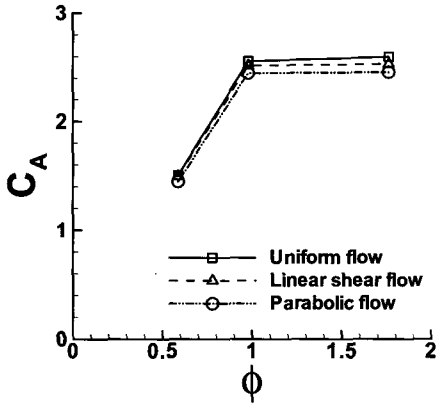

(a) Input coefficient, C_A

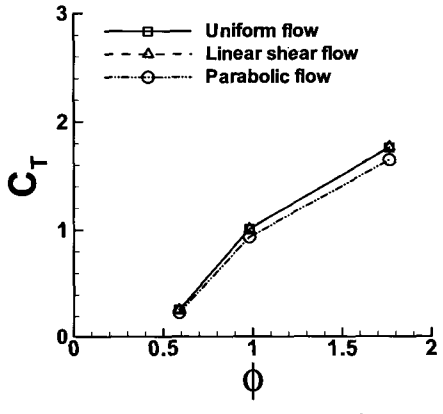

(b) Torque coefficient, C_T

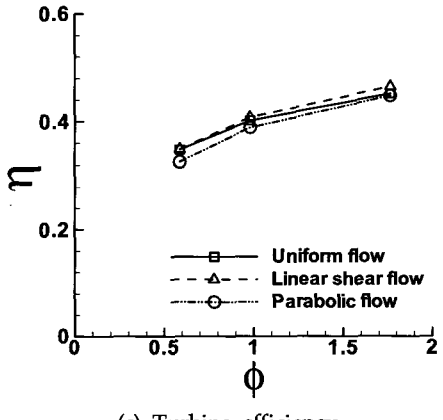

(c) Turbine efficiency, η

Fig. 10 Effect of inflow condition

(1) Flow analysis at a high Reynolds number was made for a prototype turbine, and a series of performance charts was constructed to estimate the size and performance of 250 kW-class turbines. Steady analysis was made with mean axial inflow without any effect of flow non-uniformity or unsteadiness.

(2) Quasi-steady analysis in sinusoidal inflow conditions was made for a turbine rotor, and results were compared to those of steady analysis. The difference between the two methods was found to be relatively small.

(3) Unsteady flow analysis was performed for the flow field in the air flow passage, including the OWC chamber and duct in the absence of turbine rotor, and compared to the steady case to determine that the effect of flow unsteadiness is rather minor inside a duct, although its effect is significant inside the air chamber. The effect of flow non-uniformity at the duct inlet was also considered to be negligible.

(4) A relatively simple steady flow analysis still provides the most practically useful and effective way to predict the design and performance of turbines using a series of performance chart.

Acknowledgements

This research was performed as a part of the project titled "Development of Wave Energy Utilization Technology" supported by the Ministry of Marine Affairs and Fisheries (MOMAF), Korea.

References

Hong, K. (2005), "Development of Wave Energy Utilization Technology (III)", Research Report of MOERI, Korea (in Korean).

Hong, S.W. (2004), "Development of Wave Energy Utilization Technology (II)", Research Report of KRISO, Korea (in Korean).

Hyun, B.S. and Moon, J.S. (2004), "Analysis of Impulse Turbine for Wave Energy Conversion Using CFD Method", Trans. KCORE, Vol 18, No 5, pp 1-6 (in Korean).

Hyun, B.S., Suh, J.C. and Lee, P.M. (1992), "Investigations on the Aerodynamic Aspects of Wells Turbine in a Reciprocating Flow", Proc. Second ISOPE Conf., San Francisco, USA, June 14-19, 1992.

Setoguchi, T., Santhakumar, S., Maeda, H., Takao, M. and

Kaneko, K. (2001), "A Review of Impulse Turbine for Wave Energy Conversion", Renewable Energy, Vol 23, pp 261-292.

Setoguchi, T., Kim, T.H., Kaneko, K., Takao M., Lee, Y.W. and Inoue, M. (2003), "Air Turbine with Staggered Blades for Wave Power Conversion", IJOPE, Vol 13, No 4, pp 316-320.

Thakker, A. and Hourigan, F. (2004), "Modeling and Scaling of the Impulse Turbine for Wave Power Applications", Renewable Energy 29, Elsevier, pp 305-317.

2007년 7월 9일 원고 접수
2007년 10월 15일 최종 수정본 채택